

## Exomoons of Circumbinary Planets

BEN R. GORDON,<sup>1</sup> HELENA BUSCHERMÖHLE,<sup>1</sup> WATA TUBTHONG,<sup>1</sup> DAVID V. MARTIN,<sup>1</sup> SEAN SMALLETS,<sup>1</sup>  
GRACE MASIELLO,<sup>1</sup> AND LIZ BERGERON<sup>1</sup>

<sup>1</sup>*Department of Physics & Astronomy, Tufts Astronomy, 574 Boston Avenue, Medford, MA, USA*

### ABSTRACT

Exomoon discovery is on the horizon. Although several exomoon candidates exist around single stars, there are currently no candidates around circumbinary planets (CBPs). Circumbinary planets are predicted to have migrated to their current location from a farther region of the protoplanetary disc where they formed. An exomoon of a CBP therefore represents a fascinating yet complex and evolving four-body system. Their existence (or absence) would shed light on the robustness of moon formation in more dynamically active planetary systems. In this work, we simulate exomoons around migrating CBPs. We show that for fully migrated CBPs a moon is capable of surviving the migration if it is formed within  $\sim 5 - 10\%$  of the planet's Hill Radius. Roughly 30 – 40% of the surviving moons are in the habitable zone, giving credence to circumbinary habitability even if the known CBPs all gas giants. The majority of moons fall off of their host planet early in the migration and become long-period CBPs (i.e a multi-planet circumbinary system). A subset of exomoons are ejected from the system entirely. This last class presents a new mechanism for producing free-floating planetary mass objects, like those discovered recently and expected in the Roman microlensing survey.

### 1. INTRODUCTION

There are  $> 6000$  confirmed exoplanets and a further  $> 7000$  candidates<sup>1</sup>. However, not a single exomoon has been confirmed. This is in spite of a few candidates from Kepler data (Kipping et al. 2012; Teachey & Kipping 2018; Fox & Wiegert 2021), ongoing work with the James Webb Space Telescope (Christiaens et al. 2024) and CHEOPS (Ehrenreich et al. 2023), and proposed work with The Nancy Grace Roman Space Telescope (Bachelet et al. 2022).

Exomoon detection would be extraordinary for a variety of reasons. First, more discoveries in more diverse stellar and planetary environments are needed to properly constrain formation theories. The leading theories for The Moon are the giant impactor hypothesis (Cameron & Ward 1976; Dauphas 2017) and the high energy impact model (Cuk & Stewart 2012; Pahlevan & Stevenson 2007). Moon formation models that do not inherently involve an impact include gravitational capture (Agnor & Hamilton 2006) and circumplanetary disc formation (Canup & Ward 2006; Benisty et al. 2021), the latter of which is often used to describe the formation of the large moons of Jupiter.

Exomoons may also play a role in our search for “habitable worlds”. Europa and Enceladus have long been discussed with respect to Solar System searches for life (Hand et al. 2022; Wang & Qin 2024; Souček et al. 2024). Furthermore, our moon plays a key role in the maintenance of life on Earth through control over various processes such as creating oceanic tides, shielding the Earth from asteroid collisions and regulating the Earth's spin axis (Lissauer et al. 2012).

A planet's Hill radius, within which it could potentially form and maintain Moons, scales linearly with the planet's semi-major axis (see Sect. 2.2). Therefore, it would be beneficial to search for moons around longer-period planets. This is challenging since the most prolific exoplanet discovery technique - transits - is heavily biased towards short-period planets. One creative avenue is to look for moons around circumbinary planets (CBPs). These planets are typically found at “long” periods, at least relative to the rest of the transiting population (see Fig. 1). This is due to a combination of observational biases (Martin & Triaud 2014, 2015) and planet formation restrictions (Paardekooper et al. 2012; Pierens & Nelson 2013; Martin et al. 2015; Muñoz & Lai 2015). Furthermore, a significant fraction of confirmed CBPs orbit within the habitable zone (Socia et al. 2020; Welsh et al. 2015; Orosz et al. 2019; Kostov et al. 2016b; Eggl 2018). All of the known CBPs are gas gi-

Corresponding author: Benjamin.Gordon664822@tufts.edu

<sup>1</sup> See <https://exoplanetarchive.ipac.caltech.edu/>

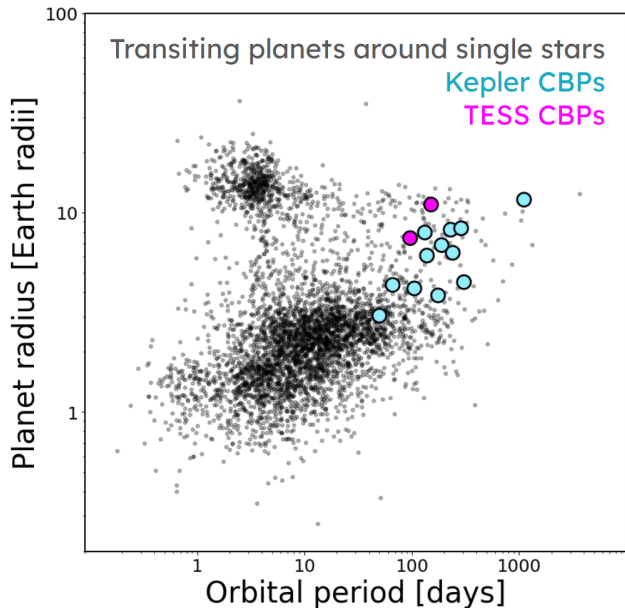


**Figure 1.** Radius and orbital period of all confirmed transiting planets (black dots), compared with the 12 Kepler (blue circles) and 2 TESS (pink circles) circumbinary planets.

ants ( $R_p > 3R_\oplus$ , Fig. 1). This might be simply an observational bias (Martin & Fabrycky 2021), but we are nevertheless motivated to search for exomoons as they may be the best chance for CBP habitability.

Most of the known CBPs orbit roughly as close as possible to the binary without being unstable. This could pose challenges for the existence of a stable exomoon. Hamers et al. (2018) showed that the known CBPs could host an exomoon, as long as it was on a close to coplanar orbit. However, that study did not consider that the planet (and its moon) likely did not form in their current location. The leading theory for CBP formation is that they did not form in situ (Paardekooper et al. 2012), but rather formed farther out in the disc before migrating in (Pierens & Nelson 2013). An exomoon around a CBP would therefore represent a dynamically evolving, close to instability, four-body system. A natural question arises: *can circumbinary exomoons survive??*

This work investigates the evolution and stability of circumbinary exomoons accounting for the effects of disc-driven planetary migration. First, we will motivate key concepts that influence the dynamics of our solar systems and summarize the three archetypal outcomes (Sect. 2). Next, we describe all parameter inputs used to synthesize unique binary-planet-moon populations (Sect. 3). After this, we present the results of our N-body simulations (Sect. 4) and offer analysis alongside future implications (Sect. 5), before concluding (Sect. 6).

## 2. FUNDAMENTAL CONCEPTS

### 2.1. Type 1 Migration

Of the 14 transiting CBPs, the majority are close to the stability limit around their binary. The stability limit roughly coincides with where the inner edge of the protoplanetary disc would have been, i.e. the binary carved out an inner “hole” (Artymowicz & Lubow 1994; Holman & Wiegert 1999; Kutra et al. 2024). It is believed that CBPs did not form in situ because the protoplanetary disc would have been too turbulent this close to the binary (Paardekooper et al. 2012). The leading theory is that they instead formed farther out before migrating inwards and then parked near the disc edge, where they are currently seen (Pierens & Nelson 2008, 2013; Penzlin et al. 2021; Martin & Fitzmaurice 2022).

Broadly speaking, there are two regimes of disc-driven migration. Type 1 migration, which we believe the known CBPs followed, comes from an exchange of angular momentum between the migrating body and a protoplanetary disc via a torque (Ward 1997). To first order, the planet does not significantly alter the structure of the disc. The structure of the disc directly influences migration as it’s an interchange between two main agents: the Lindblad and the co-rotational torques. Lindblad torque is a product of density perturbations arising from Lindblad resonances between the planet and the disc gas. In the context of a circumbinary disc, this torque is what causes a planet to lose angular momentum, pushing it inwards towards the binary.

Lubow & Ida (2010) model the Lindblad torque in Type 1 migration by:

$$T_L = -\Sigma_d \Omega^2 a^4 \left( \frac{m}{M_A + M_B} \right)^2 \left( \frac{a}{H} \right)^2, \quad (1)$$

where  $\Sigma_d$  is the density of the disc,  $m$  is the mass of the migrating planet,  $M_A$  and  $M_B$  are the masses of the primary and secondary star respectively, and  $H$  is the disc height. A typical disc height prescription is given as  $H = ha$ , where  $h$  is a scaling constant, taken to be  $h = 0.04$ , which corresponds to the surface density of a minimum mass solar nebula (MMSN) of  $\Sigma_0 = 1700k \text{ g/cm}^2$  with  $k = 1$ . The Keplerian orbital frequency,  $\Omega$ , is given by

$$\Omega = \sqrt{\frac{G(M_A + M_B)}{a^3}}, \quad (2)$$

where  $G$  is the gravitational constant. The rate at which the semi-major axis of an object decreases over time is given by the following:

$$a = a_0 \exp\left(\frac{-t}{\tau_a}\right), \quad (3)$$

where  $a_0$  is the initial semi-major axis of the object and  $\tau_a$  is the migration timescale, which is calculated according to:

$$\tau_a = \frac{J}{T_L}, \quad (4)$$

where  $T_L$  is the Lindblad torque given by Eq. 1 and  $J = m\sqrt{aGM_{\text{tot}}}$  is the object's angular momentum. A consequence of these equations is that  $\tau_a \propto 1/(\Sigma_d m)$ , i.e. migration is faster with more massive planets and denser discs.

Whilst the Lindblad torque acts to drive a planet or moon inward, the co-rotational (or horseshoe) torque does the opposite. As the disc material nearest to the planet librates with the co-orbital horseshoe region, the resulting torque pushes the planet outwards. A key difference with the Lindblad torque is that the Lindblad torque is proportional to the *disc density*, whereas the corotational torque is proportional to the *disc density gradient*, i.e.  $T_{\text{co}} \propto d\Sigma_d/dr$ . This means that nonhomogeneous regions of the disc are sources of outward forcing. In the case of binaries, there is a sharp drop-off in the density of the planetary disc arising from their orbit. At the 'inner disc edge', the co-rotational torque becomes large enough to match the Lindblad torque and cease the planet's migration.

The truncation radius of the disc, where the planet parks, roughly scales with the 'stability limit' around the binary:

$$\frac{a_s}{a_{\text{bin}}} = 1.60 + 5.10e - 2.22e^2 + 4.12\mu - 4.27e\mu - 5.09\mu^2 + 4.61e^2\mu^2, \quad (5)$$

in which  $a_s$  is the stability limit measured from the barycenter,  $e$  is the eccentricity of the binary, and  $\mu$  is the normalized reduced mass of the binary, given by  $\mu = M_A/(M_A + M_B)$  (Holman & Wiegert 1999). For reference, a binary with  $e = 0$  and  $\mu = 0.5$  yields  $a_s = 2.39a_{\text{bin}}$ .

Although the idea of a stability limit is useful in helping to conceptualize possible orbital configurations within a circumbinary system, it is not a rigid limit. Other factors, such as the planet's orbital eccentricity, orientation, phase of the orbits and mean motion resonances influence the overall stability (Doolin & Blundell 2011). To conservatively account for these complexities, we chose to set the inner disc edge of the migrating object 1.5 times the calculated stability limit, to ensure the planet would always survive the migration.

This paradigm of CBPs forming farther out, following Type 1 migration inwards then parking at the disc truncation due to a Lindblad/co-rotation torque balance,

has been established by various hydrodynamic studies (Pierens & Nelson 2008, 2013; Penzlin et al. 2021) and seems to match observed trends (Martin & Triaud 2014; Martin et al. 2015; Muñoz & Lai 2015). Even though these planets are gas giants, it is argued that they still follow Type 1 migration, and not Type 2 migration where a more massive planet clears out a gap in the disc. The argument, first put forward by Pierens & Nelson (2008), is that a CBP following Type 2 migration would not have a co-rotation torque to brake the inwards migration at the disc edge, because the horseshoe region of the disc has been cleared out. Such planets would migrate too close to the binary and be ejected. Whilst the mass division between Type 1 and 2 migration is uncertain, as are the measured masses of most of the CBPs, we follow the paradigm of Type 1 migration + parking for this work.

In our study, we implement migration using REBOUNDX (Tamayo et al. 2020), which contains add-ons to the REBOUND N-body integrator (Rein & Liu 2012; Rein & Spiegel 2015). Our implementation is similar to recent studies Martin & Fitzmaurice (2022); Fitzmaurice et al. (2022) except for two simplifications. First, we use the newly-released INNER DISC EDGE functionality of REBOUNDX to halt migration. Second, for a given circumbinary system we use a constant migration rate, calculated from Eqs. 1 and 4 at 1 AU. In a more realistic simulation, the torque would change with the migration of the planet. However, this was found to be computationally expensive for our large suite of million-year simulations. Given the migration will change by orders of magnitude between simulations of different disc densities and planet mass, we found this simplification to be acceptable.

In all of our simulations, if the moon is bound to a planet then it does not experience migration relative to the planet, since tidal or spin-induced migration will occur over a much longer timeframe than migration of the planet. The moon simply migrates with the planet. If the moon instead becomes a planet in its own right (described in Sect. 2.2), then it will follow standard independent Type 1 migration.

## 2.2. The Hill Sphere

The Hill sphere of an orbiting body is the region around it where its gravitational influence dominates over the tidal forces of the central primary body. Within this region, the orbiting body can retain moons. The Hill radius,  $r_H$ , which represents the approximate boundary of this sphere, is given by:

$$r_H = a_p \left[ \frac{m_p}{3(m_s + m_p)} \right]^{\frac{1}{3}}. \quad (6)$$

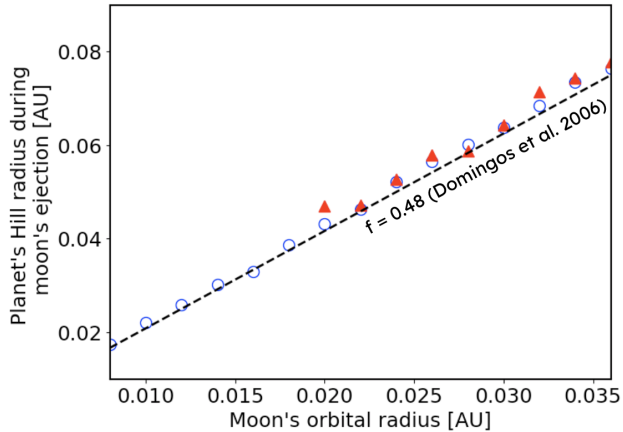


**Figure 2.** The Hill radius of the planet decreases proportionally to the distance from the binary. Plotting the planet’s Hill radius against the moon’s semi-major axis gives insight into the fraction of the Hill radius the moon is ejected from the planet. The blue dots represent the results for a single star system as presented in Domingos et al. (2006) for a star of  $1 M_{\odot}$ , and the red triangles are results for a binary system, where both stars have a combined mass of  $1 M_{\odot}$ . Both results are run for the same system. For any given orbital radius, the moon is always ejected at  $0.48 r_H$ .

In the context of our system, the Hill radius of the planet decreases as it migrates inwards. Therefore, the survivability of the moon is directly influenced by how much the Hill radius shrinks. It was shown in Domingos et al. (2006) that a prograde satellite will “fall off” at a fraction of 0.48 of the Hill radius for a single star system as the host planet undergoes type 1 migration. For ease of reference, we will define a parameter  $\gamma$ :

$$\gamma = \frac{a_m}{r_H}. \quad (7)$$

When  $\gamma \geq 0.48$ , the moon will leave its host’s sphere of gravitational influence. At this point, it either becomes a stable planet in its own right - a “ploonet”, or it is ejected entirely from the system. In Fig 2, we show that a moon around a migrating CBP will fall off at the same value of  $\gamma = 0.48$  as the single star case.

The outcome of the moon is highly sensitive to the parameter space that dictates  $r_H$  and  $a_m$ , which is large. Sect. 4 shows the interplay between the parameters in this space.

Finally, the planet’s Hill Radius, and by consequence the survivability of the moon, is also sensitive to the binary’s stability limit, although in an implicit way. The truncation radius (roughly the stability limit) is determined by the binary period, mass-ratio, and eccentricity (Eq. 5). Since the truncation radius is the inner limit of

the planet’s migration, a tighter truncation means the Hill radius shrinks more, and hence  $\gamma$  increases more. Therefore, the smaller the stability limit (roughly equivalent to saying the shorter-period the binary), the higher the chances of the moon being ejected. Results in Sect. 4 show the relationship between the binary and moon periods and the outcome of the system.

### 3. POPULATION SYNTHESIS

The four-body orbital evolution is chaotic and therefore highly sensitive to initial conditions. The demographics of circumbinary planets, particularly at their birth, are also very uncertain. To account for this, we utilize a broad population synthesis study. Here, we generate initial parameters for the Binary-Planet-Moon system as well as for the protoplanetary disc. We do this via Monte Carlo sampling of reasonable values in the following way. The primary star mass was sampled uniformly from the current distribution of binaries that host CBPs ( $1.53 M_{\odot}$  to  $0.69 M_{\odot}$ ). To calculate the secondary star mass, we sampled the mass ratio uniformly between 0.1 to 1. If this produced a mass below the stellar mass threshold ( $0.08 M_{\odot}$ ), we substituted  $0.19 M_{\odot}$ , which is the lowest mass known star to host a CBP. We sample the binary period from the Kepler binary period distribution from the smallest CBP hosting binary to the largest (from 7 to 41 days). The binary eccentricity is drawn from a Rayleigh distribution centered on the mean value of all known binaries if  $P_{\text{bin}} \geq 12$  days, and 0 otherwise.

We sample the planet’s mass by first drawing uniformly from the radii distribution for all currently known exoplanets. We then calculate a planetary mass by applying the mass-radius relationship found in Chen & Kipping (2016). A second population of planetary masses is sampled by only selecting radii greater than  $3R_{\oplus}$  to emulate the presently observed CBP population. We also place a cap on the planet’s mass at  $104.84 M_{\oplus}$  (the mass of Kepler-16) to remove all planets that may undergo type-II migration. The planet’s starting semi-major axis is uniformly sampled from 1 to 5 AU about the barycenter. If the 4:1 period resonance with the calculated stability limit is beyond 1 AU, this was then set as the lower limit, as destabilizing resonances could prevent planet/moon formation in this region (Martin & Fitzmaurice 2022).

Since we would be more likely to observe a large exomoon, we use the mass and radius of Ganymede as a constant for all calculations. The lunar semi-major axis is sampled uniformly from the Roche limit to 0.48 of the planet’s initial Hill radius. True anomaly and argument of periapsis were sampled uniformly from 0 to 360 de-

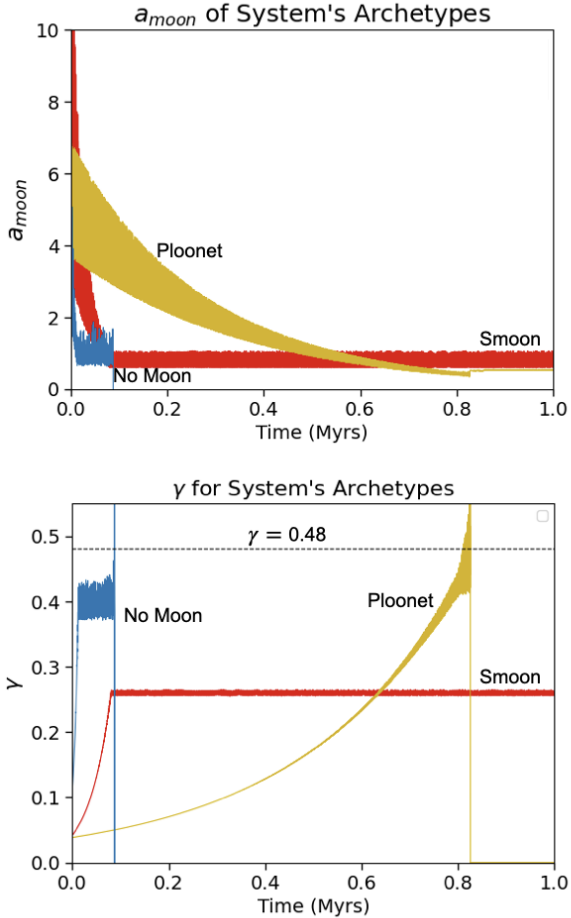


**Figure 3. Top:** Semi-major axis of the moon with respect to the binary for three archetypal systems: a saved moon (“smoon”, red), a moon-turned-planet (“ploonet”, yellow) and a completely ejected moon (“no moon”, blue). Since the osculating semi-major axis of the moon is calculated relative to the binary, the thick parts of the plot correspond to when the moon is still orbiting the planet. The ploonet example shows a moon that is initially orbiting the planet but is then dropped off and starts to orbit the binary as a planet **Bottom:**  $\gamma = a_m/r_H$  over time for the same three archetypal systems. For the saved moon (red)  $\gamma$  initially increases due to the planets migrating, before plateauing at  $\gamma \approx 0.26$  as the planet has parked at the disc edge. For the ploonet (yellow)  $\gamma$  stops being defined once it hits 0.48 and the moon is dropped off and becomes a planet in its own right. For the ejected moon (blue)  $\gamma$  is no longer defined once it is ejected from the system.

grees for both the planet and the moon. Since a typical moon’s mass is 2-3 orders of magnitude smaller than a planet, we set it as a test particle (massless particle) in the N-body simulations to save computational time. The only effect of the moon’s mass is to dictate its Type 1 migration speed if it turns into a planet.

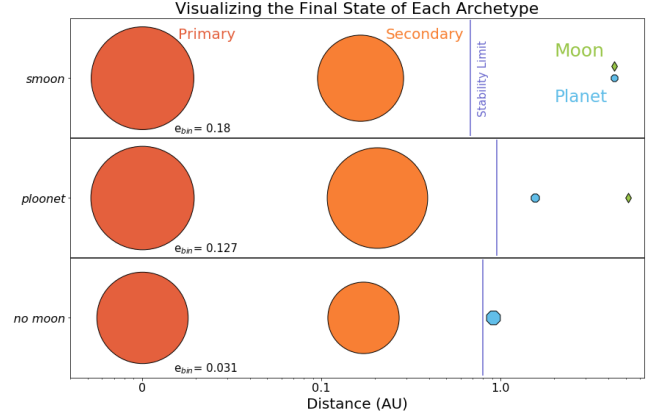


**Figure 4.** Three example simulations demonstrating a saved moon, aka “smoon” (top), a moon-turned-planet, aka “ploonet” (middle) and an ejected moon, aka “no moon” (bottom). The distance scale is logarithmic. The sizes of each circle are scaled by the body’s mass, except for the moon which is depicted as a diamond. The stability limit pictured is 1.5 times the limit calculated via criteria in Holman & Wiegert (1999).

The stability limit of the binary is calculated from Eq. 5. We multiply this by 1.5 to calculate the disc truncation radius. The migration rate of the planet is using Eq. 4, and the damping of eccentricity is found via

$$\tau_e = \frac{\tau_a}{K} \quad (8)$$

where  $K = 10$  is a constant found in Kley et al. (2004) and used in Martin & Fitzmaurice (2022).

From 1, the Lindblad is proportional to the disc surface density. We scale this surface density linearly by a factor  $k$ , which is sampled from a log uniform distribution from -2 to 2. Based on the findings in (Kraus et al. 2012; Barenfeld et al. 2019), we use a value of 1 Myr for the disc lifetime, after which the disc dissipates and there is no longer inward forcing on the migrating object.

As mentioned in Sect. 2.1, we use the REBOUND N-body code (Rein & Liu 2012) to perform N-body integration of our systems using IAS15 (Rein & Spiegel 2015), a 15th order Gauss-Radau integrator. A timestep of 100 years was used. We employ the REBOUNDx library to incorporate the effects of planetary migration (Papaloizou & Larwood 2000; Kostov et al. 2016a) and the inner disc edge (Pichierri et al. 2018; Kajtazi et al. 2023).

## 4. RESULTS

We run the N-body integrator to simulate the orbital evolution of two populations of circumbinary planets and exomoons:

- **Population 1:** No limit on planet radius.
- **Population 2:** A cut of  $R_p > 3R_\oplus$  to match the observed population of circumbinary planets, which is presently limited to large planets.

We simulated 390 systems within Population 1 and 484 within Population 2. In Sect. 4.1 we outline the three broad categories of outcomes. In Sects. 4.2 and 4.3 we discuss the results as a function of the moon orbit and the planet/star masses, respectively. The occurrence rate of each outcome is cataloged in Table 1.

#### 4.1. System Archetypes

N-body simulations yield three main outcomes for the binary-planet-moon system.

1. **Smooon:** If the moon is well within the Hill radius ( $\gamma < 0.48$ ) of the planet throughout the entirety of the migration, the planet will retain its moon, leading to a single planet system with a moon. This system will be referred to as the successful moon, or the ‘smooon’ scenario for short. See the red curves in Fig. 3 and the top example in Fig. 4.
2. **Ploonet:** During the planet’s migration, the shrinking of its Hill radius causes the moon to be “dropped off” when  $\gamma > 0.48$ . The body, formally known as a moon, is now a planet in its own right. We adopted the term ‘ploonet’ for the moon-turned-planets, following Alvarado-Montes et al. (2017) and Sucerquia et al. (2019). The ploonet interacts with the disc and undergoes Type-1 migration. Its migration speed is much slower than that of the original planet, since  $\tau_a \propto 1/m$ . Since the migration is so slow, many of the ploonets are on a wide orbit at the end of the simulation, far from the binary and planet. In some very rare cases, the moon can migrate in and get locked in an exterior mean motion resonance, similar to what was seen in Fitzmaurice et al. (2022). See the yellow curves in Fig. 3 and the middle example in Fig. 4.
3. **No moon:** The moon is entirely ejected from the system, leaving behind a single, moonless circumbinary planet. This scenario typically occurs if  $\gamma$  becomes larger than 0.48 when the planet is already quite close to the stability limit (approximately  $P_p \leq 4P_{\text{disc}}$ ). In this case, the moon cannot turn into a stable ploonet due to destabilizing and overlapping resonances relative to both the planet and the binary. See the blue curves in Fig. 3 and the bottom example in Fig. 4.

For a given starting planet and moon, and an assumption that the planet has time to migrate to the disc’s edge, one can typically predict the outcome for the moon based on a flowchart shown in 5). Some planets will not migrate to the disc edge within the 1 million-year simulation time. This is often the case for low-mass planets in low-density discs. Such cases increase the likelihood of a smooon, because the Hill radius does not shrink as far.

#### 4.2. Dependency on Moon Orbit

The distribution of  $\gamma_{\text{init}}$  versus the binary stars’ orbital radius sampled for each planetary population, color-coded by the moon’s final outcome is shown in Fig. 6, 7. General trends of the outcome are as follows. Moons with small initial  $\gamma$  are more likely to remain a satellite of their host planet. This is the case for moons in tight orbits around their host planets, since the ratio between their orbital radius to the planet’s Hill radius never exceeds the threshold  $\gamma = 0.48$ . The initial  $\gamma$  ratio that allows the moon to end up as a smooon also increases with the binary stars’ separation. This is because the planets in wide binary star systems end their migration at a larger distance from the binary stars. Thus, their final Hill radius is large, which allows moons in a wider orbit to remain in a stable orbit as the planets’ satellites. This is consistent across both planet populations.

The key difference between smooons in population 1 (all  $R_p$ ) and population 2 ( $R_p > 3R_\oplus$ ) is that the presence of small planets in the first population leads to smooons with larger orbital radii. These can be seen from the sparse red dots with  $\gamma_{\text{init}} > 0.1$  in the first planet population in Fig.6, that are not present in the CBP population (Fig.7). This is due to the planet’s migration timescale, which is proportional to the planet’s mass (Eq. 4). In our simulations, the calculated planetary migration timescale ranges from 10 kyr to 25 Myr. Under the assumption that the disc lifetime is finite, small planets that migrate slowly will not be able to reach the inner disc edge before the disc dissipates. These small planets settle in wide orbits around the binary stars, resulting in a larger Hill radius. As a result, they retain their moons as satellites. This type of binary-planet-moon system does not exist in the second population ( $R_p > 3R_\oplus$ ), as the planets in these planets generally migrate quickly enough to reach the inner disc edge before the disc dissipates.

The majority of planets in our simulations do not retain their moons. As mentioned in Sect. 4.1, moons that leave the Hill sphere of the planet close to the end of the planet’s migration are likely to end up in an unstable orbit and will eventually be ejected. A few cases of

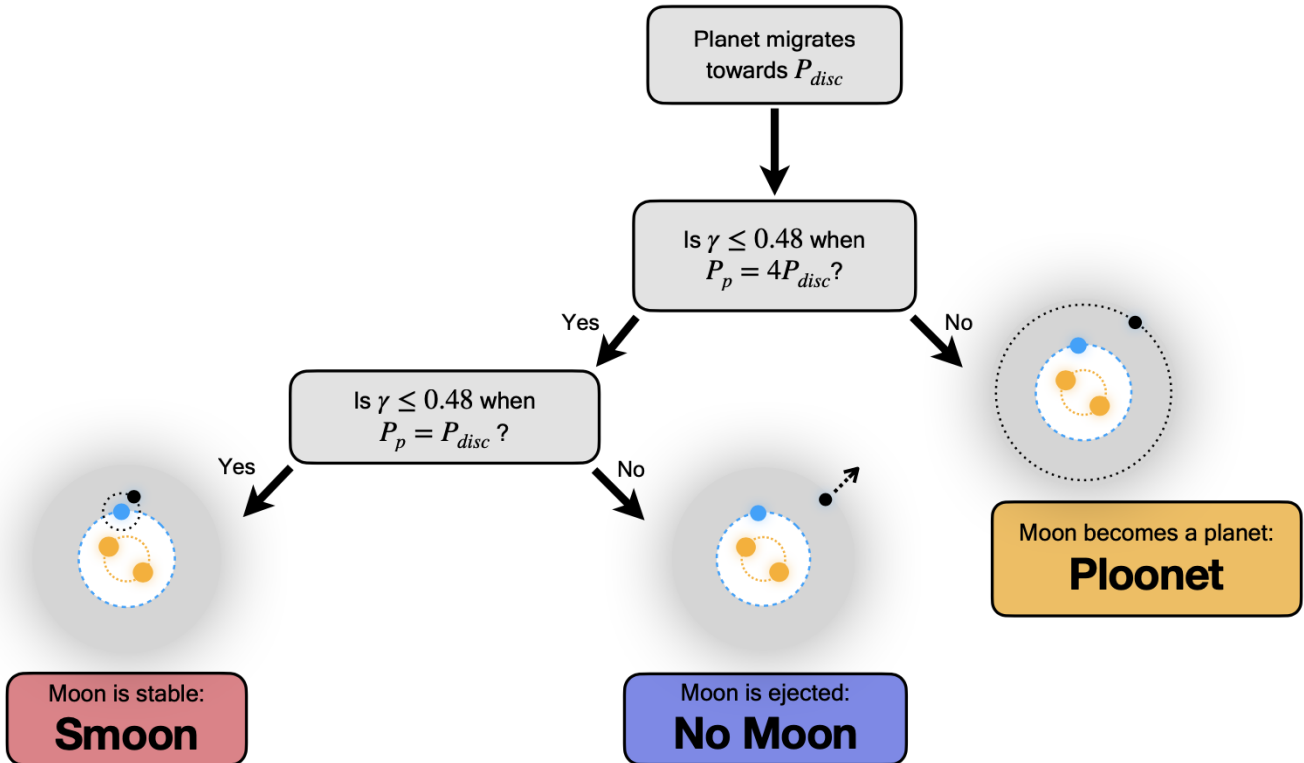


**Figure 5.** Flowchart showing the three expected outcomes of a moon orbiting a circumbinary planet that migrates in towards the inner edge of a circumbinary disc ( $P_{disc}$ ), as described in Sect. 4.1. If the planet does not migrate all the way to the disk edge then the moon is more likely to be saved (a “smooon”).

**Table 1.** The occurrence rate of each outcome of 4 different simulations with differing planet and moon masses. The primary simulations, with a Ganymede mass moon, are the top two rows: Population 1 (all  $R_p$ ) and Population 2 ( $R_p > 3R_\oplus$ ). In the bottom two rows we make the moon much more massive (Earth mass) to test the effect of faster migration.

Population	Moon Mass ( $M_\oplus$ )	Ploonets (%)	Smooons (%)	No Moon (%)
All $R_p$	0.025	258 (66.15)	119 (30.51)	13 (3.33)
$R_p < 3R_\oplus$	0.025	390 (80.58)	70 (14.46)	24 (4.96)
All $R_p$	1	301 (72.01)	101 (24.16)	16 (3.83)
$R_p < 3R_\oplus$	1	392 (85.22)	46 (10)	22 (4.78)

such outcome were observed in our simulations (the “no moon” archetypes). Most of these systems occupy the intermediate region between the smooon and the ploonets in the  $\gamma_{init} - a_{bin}$  space.

Ploonets, the case in which  $\gamma_{init}$  is large, had the highest occurrence rate of all outcomes. As previously discussed in Sect. 4.1, moons that leave the planet’s Hill sphere whilst still far from the binary are the most likely to remain stable. In Fig. 9 we histogram the period of the surviving ploonets. Most of them are on multi-year periods. This is because the moons in our sample are

approximately 1 to 5 orders of magnitude less massive than the planet, with a migration timescale on the order of 10 to 100 Myr. These migration timescales are much smaller than the 1 Myr lifetime of the disc, so ploonets hardly migrate from where they were dropped off. If the ploonet migrated faster (or for longer) then it could be trapped in an exterior mean motion resonance with the planet, as seen in Fitzmaurice et al. (2022). However, given the slow migration of the moon in our simulations, this was a rare event.

#### 4.3. Dependence on Planet and Star Masses

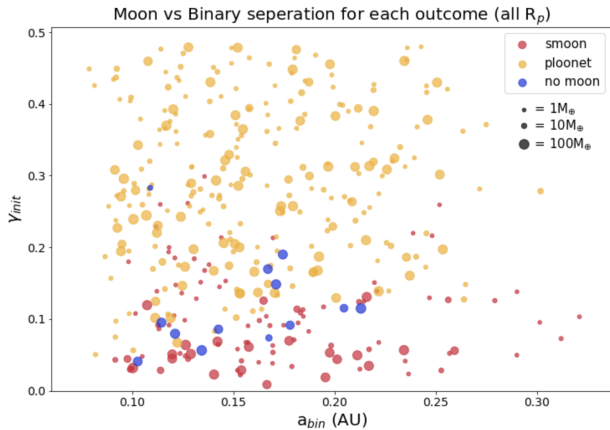


**Figure 6.** Results from the N-body simulation showing how the initial moon-planet and planet-binary separation impacts the outcome. The planet-moon, two-planet, and single-planet archetypes are labeled via blue, red, and yellow dots, respectively. The dot size corresponds to that planet’s mass on a log scale. As predicted, moons that are initially very close to their host planet are retained, whereas moons initially far from their host planet become easily unstable. The binary separation also plays a critical role, as a wider binary makes it more likely for a planet to retain its moon. Less massive planets did not migrate as far and were able to retain their moons, as seen by small red dots with a large  $\gamma_{\text{init}}$ .

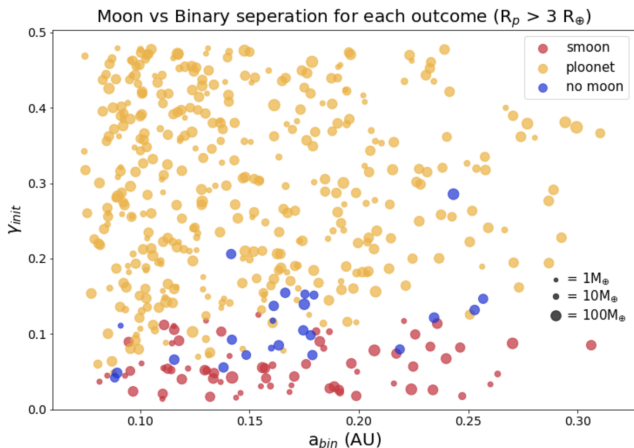


**Figure 7.** The results of N-body simulations but only with planets whose radius is larger than  $3 R_{\oplus}$ . More massive planets are able to complete their migration within the disc lifetime, eliminating the outliers seen in Fig. 6.

Figure 8 shows planetary mass plotted against the total stellar mass for all outcomes of the full planet population and CBP population combined. While the binary mass has no impact on the outcome, no moons are ejected from the system for planetary masses below the threshold of 6 earth masses. Below this threshold, a planet’s migration rate is so slow that most of them

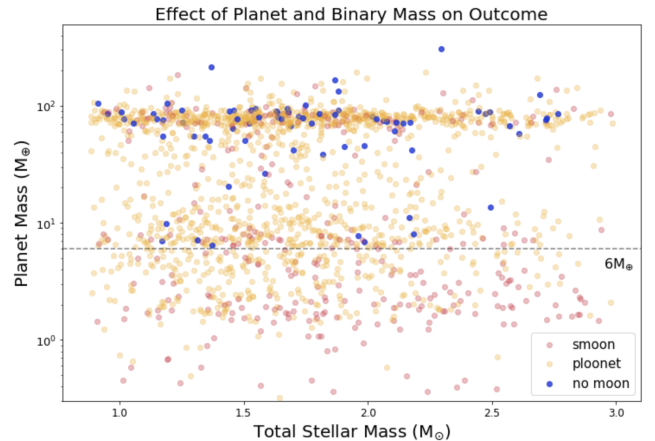


**Figure 8.** The occurrence rate of fully ejected circumbinary exomoons is elevated with increased planet mass. More massive planets migrate faster and thus are more likely to lose a moon if the moon initially resides above 5% of the planet’s Hill radius. Faster planet migration also allows more moons to be dropped off close to or within the 4:1 period resonance with the stability limit, increasing the likelihood of interactions with destabilizing resonances.

remain far from the binary stars, and are more likely to retain their moons. Planets with  $M_p > 6M_{\oplus}$  have larger Hill radii and thus retain moons that form between  $0.05 < \gamma_{\text{init}} < 0.20$  more easily compared to their smaller counterparts. These planets also have shorter migration timescales, allowing a higher occurrence of their moons to become unstable near or within the 4:1 period resonance with the stability limit, which is a prime location for destabilizing resonance (Martin & Fitzmaurice 2022).

This total ejection scenario could provide a mechanism to explain the plethora of Planetary Mass Objects (PMOs) (Osorio et al. 2000; Miret-Roig et al. 2021) seen via direct observations or microlensing missions. Alongside this, Figures 6 and 7 show that fully ejected moons are more likely for short-period binaries. Thus, PMOs may be more likely to appear near young and short-period binaries with massive planets close to the stability limit.

## 5. DISCUSSION

### 5.1. Multi-Planet Circumbinary Systems

The most likely outcome of our simulations is a ploonet (see Table 1). This is a multi-planet circumbinary system. There are two known multi-planet systems: Kepler-47 (3 transiting planets, Orosz et al. 2019) and TOI-1338/BEBOP-1 (1 transiting and 1 non-transiting planet, Kostov et al. 2020; Standing et al. 2023). These systems differ from our ploonet in three ways. First, the discovered planets are all much more



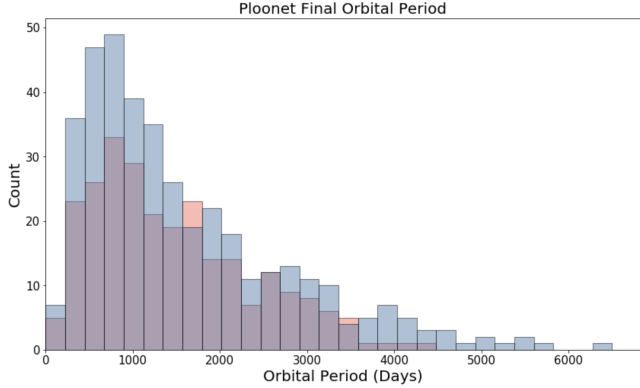


**Figure 9.** Final orbital period for all ploonets. A majority of ploonets have periods above 1000 days, larger than much of the current population of known CBPs.

massive than Earth, i.e. nothing is in the realm of a moon mass. Second, in both discovered multi-planet systems the smallest planet is on the tightest orbit, which is opposite to our ploonets. Third, most of our ploonets have a much longer period than the discovered planets, owing to a very slow Type-1 migration rate for moon-mass bodies. Figure 9 shows the final period of all ploonets for both populations of planets.

### 5.2. Habitable Zone Planets & Moons

The occurrence rate of ploonets and smoons has implications for the discussion of habitability in these systems. While it is thought that planets below  $0.3 M_{\oplus}$  cannot support atmospheric growth or plate tectonics on timescales required to harbor life (Raymond et al. 2007), it may be possible that moons of gas giants can reach earth size or larger (Teachey & Kipping 2018). For systems with earth-sized moons, we can approximate the radiant flux from the host star, and thus the surface temperature of orbiting objects in the following way:

For main sequence stars, the luminosity is related to the mass,  $M$ , of the star via

$$\frac{L}{L_{\odot}} = \left( \frac{M}{M_{\odot}} \right)^{3.5}. \quad (9)$$

We can calculate this for both stars and then add up the luminosities such that  $L_{AB} = L_A + L_B$ . From this, we can get the incoming flux,  $F_{in}$ , received by an object orbiting at a distance,  $d$ , away via

$$F_{in} = \frac{L_{AB}}{4\pi d^2}. \quad (10)$$

With this flux, we can equate the incoming energy to the energy radiated away by the object. For a spherical

body of radius  $R$ , this can be written as

$$F_{in}\pi R^2 = F_{out}4\pi R^2, \quad (11)$$

where  $F_{out} = \sigma T^4$  is the flux radiated away by the body of temperature  $T$ , according to the Stefan-Boltzmann Law. The temperature of the body then can be written in terms of the incoming stellar flux:

$$T = \left( \frac{F_{in}}{4\sigma} \right)^{\frac{1}{4}}, \quad (12)$$

where  $\sigma$  is the Stefan-Boltzmann constant. The temperature range at which water is liquid is given as 273-373 K. Objects with a surface temperature within this range will be designated as residing within the habitable zone of their host binary.

Table 2 shows the relative percentages of ploonets, smoons, and planets that reside in the habitable zone when the disk dissipates for both populations of planets. Smoons of the full planet population are 10% less likely to reside in the habitable zone than our larger planet population, as many of the small planets will take on very wide orbits, preventing liquid water from occurring.

### 5.3. Free Floating “Planets”

The Galaxy is believed to be populated by free-floating or “rogue” bodies that are not bound to a star. These could be planetary mass objects, of which some have been discovered by microlensing (Sumi et al. 2011; Clanton & Gaudi 2017), or smaller asteroid-like objects like those seen recently passing through our Solar System (e.g. ‘Oumuamua, Meech et al. 2017).

Binary stars have been touted as a potential birth environment for free-floating planets. Smullen et al. (2016); Sutherland & Fabrycky (2016) demonstrated that for unstable circumbinary planets, an ejection was much more likely than a collision with either star. Fitzmaurice et al. (2022) showed that migrating multi-planet circumbinary systems frequently eject the lower mass planet. Coleman (2024) proposed using the velocity distribution of free-floating bodies to test if they were ejected from binaries (higher velocity) or single stars (lower velocity).

In this paper, we have created another production method for free-floating bodies. In our simulations, moons are naturally ejected if they fall off the planet ( $\gamma > 0.48$ ) when the planet is reasonably close to the disc edge. Another possibility is that our simulations create a large number of ploonets, and whilst those survive our simulations, if there were another planet in the system then a low-mass ploonet would be susceptible to ejection (Fitzmaurice et al. 2022).

**Table 2.** Percentages of moons and ploonets that orbit within the habitable zone for each population of host planets. Moons of lower-mass planets occur roughly 4x more often than for the CBP population, as these small planets are not able to migrate to the disc. Moon-sized objects migrate at timescales much smaller than 1 Myr, resulting in the habitable zone ploonet percentages being similar.

Population	Ploonets (%)	Moons (%)	All Planets (%)
All $R_p$	67/301 (22.26)	33/101 (32.67)	119/418 (28.47)
$R_p < 3R_\oplus$	90/392 (22.96)	20/46 (43.48)	134/460 (29.13)

#### 5.4. Assumptions & Caveats

##### 5.4.1. Additional Planets

We assume that a single planet + moon system is created at a distance of 1-5 AU from the binary, and allowed to migrate inwards unimpeded by any other planets. The addition of other planets, in particular more massive ones, would likely lead to increased instability. A particular effect would be on ploonets, which are often dropped off at wide orbitals which could be vulnerable to destabilization by other bodies.

##### 5.4.2. Migration Timescales

There is significant uncertainty in how fast the moon will migrate after it becomes a ploonet. To test the impact of this, we reran our N-body simulations. We take the moon’s mass to be  $1 M_\oplus$ , or as 90% of the host planet’s mass if  $M_p \leq 1M_\oplus$  so that the moon does not migrate as fast as the planet. By allowing the moons to migrate faster, we increase the chance of ploonets becoming unstable by migrating too close to the planet and the binary. The results were qualitatively the same as with a Ganymede-mass moon, with only a 4 – 6% decrease in moons and a 6% increase in ploonets, depending on the population (see Table 1).

It is also assumed that the planet and moon have already formed before the simulations have started, with no accretion occurring along the way. This assumption is quite common amongst simulations of planetary migration, both hydrodynamical (Pierens & Nelson 2013) and N-body (Rein 2012; Martin & Fitzmaurice 2022).

Our N-body simulation of migration also has many assumptions and simplifications. We use a fixed migration rate, calculated based on the Lubow & Ida (2010) Lindblad torque at a somewhat arbitrary distance of 1 AU. We do not model any effects of turbulence in the disc, e.g. with stochastic forcing, although this was not seen to significantly impact the results of circumbinary planet migration in Martin & Fitzmaurice (2022).

Finally, we assume that there is no migration of the moon as a moon, due to tidal and spin interactions with the planet. Such an effect would occur over a longer timespan than the migration and hence we neglect it. We leave it to other studies (similar to Kisare & Fab-

rycky 2024) to test if our moons would remain long-term stable as the smoon evolves slowly post-migration.

##### 5.5. Coplanarity

All systems are presumed to be coplanar. This may be reasonable, given the known CBPs all have orbits that are coplanar with the binary orbit to within  $\sim 4^\circ$ , although this might be an observational bias and not representative of the entire CBP population (Martin & Triaud 2014; Li et al. 2016; Martin 2017). Misalignment of the planet and/or moon orbit could be destabilizing for the moon (Hamers et al. 2018), although we expect that during migration the protoplanetary disc would dampen inclinations. For reference, the orbital plane of The Moon is misaligned by  $\sim 5^\circ$  relative to the Earth’s orbit around The Sun. Misaligned moons could be discovered in transit, but their observational signature may pose additional complexities (Kipping 2009a,b; Martin et al. 2019).

##### 5.5.1. Population Synthesis

There is significant uncertainty in the simulated population. The binary stars are relatively well known. For the planets, we have barely more than a dozen discoveries, and with significant biases (e.g. it’s harder to find longer period and smaller planets). In addition, we are simulating the initial location of the planets, which is even more uncertain. Finally, the simulated exomoon population is likely the least certain, based solely on Solar System and Hill stability considerations. Ultimately,

## 6. OUTLOOK & CONCLUSION

Whilst there are currently no exomoon candidates around CBPs, our work shows that CBPs are capable of retaining moons through the migration process. Since CBPs are migrating within a truncated protoplanetary disc, they do not migrate in as far as planets around single stars. This means that their Hill sphere does not shrink as much, which aids their ability to retain moons. This work shows that wide binaries are more likely to host CBPs with exomoons, as binaries separated by 0.3 AU host moons initially residing at 10% of their host planet’s Hill radius, compared to 5% for binaries separated by 0.1 AU.

Our work also has implications for habitable worlds. For the known circumbinary planets, whilst they might be gas giants,  $\approx 30\%$  of them reside within the habitable zone. In our simulations across all possible planet sizes, 6% of our simulations finish with a moon in the habitable zone and 18% of our simulations finish with a ploonet in the habitable zone.

Finally, our work has implications for present and upcoming observing missions. The plausibility of habitable exomoons around CBPs may motivate JWST, CHEOPS, or similar searches for exomoons using transit and/or transit timing methods. Our simulations also have provided a new mechanism for free-floating planet production, the likes of which might be detectable by the upcoming Roman microlensing mission.

## ACKNOWLEDGEMENTS

We would like to thank various members of the astrophysics groups at Tufts University and The Ohio State University for valuable discussions that helped grow ideas within this paper. We would also like to thank our families for their unwavering support throughout our work. This work commenced in Spring 2024 as a 3-credit research course taught at Tufts University: “Special Studies in Astrophysics”. All enrolled students contributed and are featured as co-authors.

## REFERENCES

- Agnor, C. B., & Hamilton, D. P. 2006, *Nature*, 441, 192, doi: [10.1038/nature04792](https://doi.org/10.1038/nature04792)
- Alvarado-Montes, J. A., Zuluaga, J. I., & Sucerquia, M. 2017, *MNRAS*, 471, 3019, doi: [10.1093/mnras/stx1745](https://doi.org/10.1093/mnras/stx1745)
- Artymowicz, P., & Lubow, S. H. 1994, *ApJ*, 421, 651, doi: [10.1086/173679](https://doi.org/10.1086/173679)
- Bachelet, E., Specht, D., Penny, M., et al. 2022, *A&A*, 664, A136, doi: [10.1051/0004-6361/202140351](https://doi.org/10.1051/0004-6361/202140351)
- Barenfeld, S. A., Carpenter, J. M., Sargent, A. I., et al. 2019, *ApJ*, 878, 45, doi: [10.3847/1538-4357/ab1e50](https://doi.org/10.3847/1538-4357/ab1e50)
- Benisty, M., Bae, J., Facchini, S., et al. 2021, *The Astrophysical Journal Letters*, 916, L2, doi: [10.3847/2041-8213/ac0f83](https://doi.org/10.3847/2041-8213/ac0f83)
- Cameron, A. G. W., & Ward, W. R. 1976, in *Lunar and Planetary Science Conference*, Vol. 7, Lunar and Planetary Science Conference, 120
- Canup, R. M., & Ward, W. R. 2006, *Nature*, 441, 834, doi: [10.1038/nature04860](https://doi.org/10.1038/nature04860)
- Chen, J., & Kipping, D. 2016, *The Astrophysical Journal*, 834, 17, doi: [10.3847/1538-4357/834/1/17](https://doi.org/10.3847/1538-4357/834/1/17)
- Christiaens, V., Samland, M., Henning, T., et al. 2024, *A&A*, 685, L1, doi: [10.1051/0004-6361/202349089](https://doi.org/10.1051/0004-6361/202349089)
- Clanton, C., & Gaudi, B. S. 2017, *ApJ*, 834, 46, doi: [10.3847/1538-4357/834/1/46](https://doi.org/10.3847/1538-4357/834/1/46)
- Coleman, G. A. L. 2024, *MNRAS*, 530, 630, doi: [10.1093/mnras/stae903](https://doi.org/10.1093/mnras/stae903)
- Cuk, M., & Stewart, S. 2012, *Science (New York, N.Y.)*, 338, doi: [10.1126/science.1225542](https://doi.org/10.1126/science.1225542)
- Dauphas, N. 2017, *Nature*, 541, 521, <https://api.semanticscholar.org/CorpusID:205253143>
- Domingos, R. C., Winter, O. C., & Yokoyama, T. 2006, *MNRAS*, 373, 1227, doi: [10.1111/j.1365-2966.2006.11104.x](https://doi.org/10.1111/j.1365-2966.2006.11104.x)
- Doolin, S., & Blundell, K. M. 2011, *MNRAS*, 418, 2656, doi: [10.1111/j.1365-2966.2011.19657.x](https://doi.org/10.1111/j.1365-2966.2011.19657.x)
- Eggl, S. 2018, in *Handbook of Exoplanets*, ed. H. J. Deeg & J. A. Belmonte, 61, doi: [10.1007/978-3-319-55333-7\\_61](https://doi.org/10.1007/978-3-319-55333-7_61)
- Ehrenreich, D., Delrez, L., Akisanmi, B., et al. 2023, *A&A*, 671, A154, doi: [10.1051/0004-6361/202244790](https://doi.org/10.1051/0004-6361/202244790)
- Fitzmaurice, E., Martin, D. V., & Fabrycky, D. C. 2022, *MNRAS*, 512, 5023, doi: [10.1093/mnras/stac741](https://doi.org/10.1093/mnras/stac741)
- Fox, C., & Wiegert, P. 2021, *MNRAS*, 501, 2378, doi: [10.1093/mnras/staa3743](https://doi.org/10.1093/mnras/staa3743)
- Hamers, A. S., Cai, M. X., Roa, J., & Leigh, N. 2018, *MNRAS*, 480, 3800, doi: [10.1093/mnras/sty2117](https://doi.org/10.1093/mnras/sty2117)
- Hand, K. P., Phillips, C. B., Murray, A., et al. 2022, *PSJ*, 3, 22, doi: [10.3847/PSJ/ac4493](https://doi.org/10.3847/PSJ/ac4493)
- Holman, M. J., & Wiegert, P. A. 1999, *AJ*, 117, 621, doi: [10.1086/300695](https://doi.org/10.1086/300695)
- Kajtazi, K., Petit, A. C., & Johansen, A. 2023, *A&A*, 669, A44, doi: [10.1051/0004-6361/202244460](https://doi.org/10.1051/0004-6361/202244460)
- Kipping, D. M. 2009a, *MNRAS*, 392, 181, doi: [10.1111/j.1365-2966.2008.13999.x](https://doi.org/10.1111/j.1365-2966.2008.13999.x)
- . 2009b, *MNRAS*, 396, 1797, doi: [10.1111/j.1365-2966.2009.14869.x](https://doi.org/10.1111/j.1365-2966.2009.14869.x)
- Kipping, D. M., Bakos, G. Á., Buchhave, L., Nesvorný, D., & Schmitt, A. 2012, *ApJ*, 750, 115, doi: [10.1088/0004-637X/750/2/115](https://doi.org/10.1088/0004-637X/750/2/115)
- Kisare, A. M., & Fabrycky, D. C. 2024, *MNRAS*, 527, 4371, doi: [10.1093/mnras/stad3543](https://doi.org/10.1093/mnras/stad3543)
- Kley, W., Peitz, J., & Bryden, G. 2004, *A&A*, 414, 735, doi: [10.1051/0004-6361:20031589](https://doi.org/10.1051/0004-6361:20031589)
- Kostov, V. B., Moore, K., Tamayo, D., Jayawardhana, R., & Rinehart, S. A. 2016a, *ApJ*, 832, 183, doi: [10.3847/0004-637X/832/2/183](https://doi.org/10.3847/0004-637X/832/2/183)

- Kostov, V. B., Orosz, J. A., Welsh, W. F., et al. 2016b, *ApJ*, 827, 86, doi: [10.3847/0004-637X/827/1/86](https://doi.org/10.3847/0004-637X/827/1/86)
- Kostov, V. B., Orosz, J. A., Feinstein, A. D., et al. 2020, *AJ*, 159, 253, doi: [10.3847/1538-3881/ab8a48](https://doi.org/10.3847/1538-3881/ab8a48)
- Kraus, A. L., Ireland, M. J., Hillenbrand, L. A., & Martinache, F. 2012, *ApJ*, 745, 19, doi: [10.1088/0004-637X/745/1/19](https://doi.org/10.1088/0004-637X/745/1/19)
- Kutra, T., Prato, L., Tofflemire, B. M., et al. 2024, arXiv e-prints, arXiv:2411.05203, doi: [10.48550/arXiv.2411.05203](https://doi.org/10.48550/arXiv.2411.05203)
- Li, G., Holman, M. J., & Tao, M. 2016, *ApJ*, 831, 96, doi: [10.3847/0004-637X/831/1/96](https://doi.org/10.3847/0004-637X/831/1/96)
- Lissauer, J. J., Barnes, J. W., & Chambers, J. E. 2012, *Icarus*, 217, 77, doi: [10.1016/j.icarus.2011.10.013](https://doi.org/10.1016/j.icarus.2011.10.013)
- Lubow, S. H., & Ida, S. 2010, *Planet Migration*. <https://arxiv.org/abs/1004.4137>
- Martin, D. V. 2017, *MNRAS*, 465, 3235, doi: [10.1093/mnras/stw2851](https://doi.org/10.1093/mnras/stw2851)
- Martin, D. V., & Fabrycky, D. C. 2021, *AJ*, 162, 84, doi: [10.3847/1538-3881/abeab1](https://doi.org/10.3847/1538-3881/abeab1)
- Martin, D. V., Fabrycky, D. C., & Montet, B. T. 2019, *ApJL*, 875, L25, doi: [10.3847/2041-8213/ab0aea](https://doi.org/10.3847/2041-8213/ab0aea)
- Martin, D. V., & Fitzmaurice, E. 2022, *Running The Gauntlet – Survival of Small Circumbinary Planets Migrating Through Destabilising Resonances*, doi: <https://doi.org/10.1093/mnras/stac090>
- Martin, D. V., Mazeh, T., & Fabrycky, D. C. 2015, *MNRAS*, 453, 3554, doi: [10.1093/mnras/stv1870](https://doi.org/10.1093/mnras/stv1870)
- Martin, D. V., & Triaud, A. H. M. J. 2014, *A&A*, 570, A91, doi: [10.1051/0004-6361/201323112](https://doi.org/10.1051/0004-6361/201323112)
- . 2015, *MNRAS*, 449, 781, doi: [10.1093/mnras/stv121](https://doi.org/10.1093/mnras/stv121)
- Meech, K. J., Weryk, R., Micheli, M., et al. 2017, *Nature*, 552, 378, doi: [10.1038/nature25020](https://doi.org/10.1038/nature25020)
- Miret-Roig, N., Bouy, H., Raymond, S. N., et al. 2021, *Nature Astronomy*, 6, 89–97, doi: [10.1038/s41550-021-01513-x](https://doi.org/10.1038/s41550-021-01513-x)
- Muñoz, D. J., & Lai, D. 2015, *Proceedings of the National Academy of Science*, 112, 9264, doi: [10.1073/pnas.1505671112](https://doi.org/10.1073/pnas.1505671112)
- Orosz, J. A., Welsh, W. F., Haghighipour, N., et al. 2019, *AJ*, 157, 174, doi: [10.3847/1538-3881/ab0ca0](https://doi.org/10.3847/1538-3881/ab0ca0)
- Osorio, M. R. Z., Bejar, V. J. S., Martin, E. L., et al. 2000, *Science*, 290, 103, doi: [10.1126/science.290.5489.103](https://doi.org/10.1126/science.290.5489.103)
- Paardekooper, S.-J., Leinhardt, Z. M., Thébault, P., & Baruteau, C. 2012, *ApJL*, 754, L16, doi: [10.1088/2041-8205/754/1/L16](https://doi.org/10.1088/2041-8205/754/1/L16)
- Pahlevan, K., & Stevenson, D. J. 2007, *Earth and Planetary Science Letters*, 262, 438, doi: <https://doi.org/10.1016/j.epsl.2007.07.055>
- Papaloizou, J. C. B., & Larwood, J. D. 2000, *MNRAS*, 315, 823, doi: [10.1046/j.1365-8711.2000.03466.x](https://doi.org/10.1046/j.1365-8711.2000.03466.x)
- Penzlin, A. B. T., Kley, W., & Nelson, R. P. 2021, *Astronomy and Astrophysics*, 645, A68, doi: [10.1051/0004-6361/202039319](https://doi.org/10.1051/0004-6361/202039319)
- Pichierri, G., Morbidelli, A., & Crida, A. 2018, *Celestial Mechanics and Dynamical Astronomy*, 130, 54, doi: [10.1007/s10569-018-9848-2](https://doi.org/10.1007/s10569-018-9848-2)
- Pierens, A., & Nelson, R. P. 2008, *A&A*, 483, 633, doi: [10.1051/0004-6361:200809453](https://doi.org/10.1051/0004-6361:200809453)
- . 2013, *A&A*, 556, A134, doi: [10.1051/0004-6361/201321777](https://doi.org/10.1051/0004-6361/201321777)
- Raymond, S. N., Scalzo, J., & Meadows, V. S. 2007, *ApJ*, 669, 606, doi: [10.1086/521587](https://doi.org/10.1086/521587)
- Rein, H. 2012, *MNRAS*, 427, L21, doi: [10.1111/j.1745-3933.2012.01337.x](https://doi.org/10.1111/j.1745-3933.2012.01337.x)
- Rein, H., & Liu, S. F. 2012, *A&A*, 537, A128, doi: [10.1051/0004-6361/201118085](https://doi.org/10.1051/0004-6361/201118085)
- Rein, H., & Spiegel, D. S. 2015, *MNRAS*, 446, 1424, doi: [10.1093/mnras/stu2164](https://doi.org/10.1093/mnras/stu2164)
- Smullen, R. A., Kratter, K. M., & Shannon, A. 2016, *MNRAS*, 461, 1288, doi: [10.1093/mnras/stw1347](https://doi.org/10.1093/mnras/stw1347)
- Socia, Q., Welsh, W., Orosz, J., et al. 2020, *The Astronomical Journal*, doi: [10.48550/arXiv.2001.02840](https://doi.org/10.48550/arXiv.2001.02840)
- Souček, O., Běhounková, M., Lanzendörfer, M., Tobie, G., & Choblet, G. 2024, *Nature Communications*, 15, 7405, doi: [10.1038/s41467-024-51677-z](https://doi.org/10.1038/s41467-024-51677-z)
- Standing, M. R., Sairam, L., Martin, D. V., et al. 2023, *Nature Astronomy*, 7, 702, doi: [10.1038/s41550-023-01948-4](https://doi.org/10.1038/s41550-023-01948-4)
- Sucerquia, M., Alvarado-Montes, J. A., Zuluaga, J. I., Cuello, N., & Giuppone, C. 2019, *Monthly Notices of the Royal Astronomical Society*, 489, 2313–2322, doi: [10.1093/mnras/stz2110](https://doi.org/10.1093/mnras/stz2110)
- Sumi, T., Kamiya, K., Bennett, D. P., et al. 2011, *Nature*, 473, 349, doi: [10.1038/nature10092](https://doi.org/10.1038/nature10092)
- Sutherland, A. P., & Fabrycky, D. C. 2016, *ApJ*, 818, 6, doi: [10.3847/0004-637X/818/1/6](https://doi.org/10.3847/0004-637X/818/1/6)
- Tamayo, D., Rein, H., Shi, P., & Hernandez, D. M. 2020, *MNRAS*, 491, 2885, doi: [10.1093/mnras/stz2870](https://doi.org/10.1093/mnras/stz2870)
- Teachey, A., & Kipping, D. M. 2018, *Science Advances*, 4, doi: [10.1126/sciadv.aav1784](https://doi.org/10.1126/sciadv.aav1784)
- Wang, B., & Qin, H. 2024, *Science China Earth Sciences*, 67, 3515, doi: [10.1007/s11430-023-1390-6](https://doi.org/10.1007/s11430-023-1390-6)
- Ward, W. R. 1997, *Icarus*, 126, 261, doi: [10.1006/icar.1996.5647](https://doi.org/10.1006/icar.1996.5647)
- Welsh, W. F., Orosz, J. A., Short, D. R., et al. 2015, *ApJ*, 809, 26, doi: [10.1088/0004-637X/809/1/26](https://doi.org/10.1088/0004-637X/809/1/26)